

**CROSS SECTIONS FOR IONIZATION IN COLLISIONS  
BETWEEN EXCITED NITROGEN MOLECULES  
AND ARGON ATOMS, OXYGEN MOLECULES,  
AND NITRIC OXIDE MOLECULES**

By  
Nyle G. Utterback and Bert VanZyl

DECEMBER 1968

Distribution of this report is provided in the interest of information exchange.  
Responsibility for the contents resides in the author or organization that prepared it.

Prepared under  
Contract No. NAS2-4924

by  
AC ELECTRONICS-DEFENSE RESEARCH LABORATORIES

General Motors Corporation  
Santa Barbara, California  
(AC-DRL Report No. TR68-65)

for  
AMES RESEARCH CENTER  
NATIONAL AERONAUTICS and SPACE ADMINISTRATION

CROSS SECTIONS FOR IONIZATION IN COLLISIONS BETWEEN  
EXCITED NITROGEN MOLECULES AND ARGON ATOMS,  
OXYGEN MOLECULES, AND NITRIC OXIDE MOLECULES

by

Nyle G. Utterback and Bert Van Zyl

SUMMARY

A molecular beam of  $N_2$  in the  $A^3\Sigma_u^+$  state has been used to bombard target molecules of Ar,  $O_2$ , and NO. The ionization cross sections have been determined for these collisions at kinetic energies from a few eV above the energy threshold to 100 eV above threshold in the center-of-mass coordinate system. Preliminary measurements of the cross section involving CO target molecules have also been made. A comparison of all these cross-section values with those obtained using ground-state  $N_2$  molecules indicates that internal electronic energy is roughly equivalent to an equal amount of kinetic energy in producing ionization by a given ionizing process. However, certain selection rules appear to limit the ionizing processes which can occur, thereby decreasing the total cross section in some cases at a given kinetic-plus-internal energy.



## CONTENTS

<u>Section</u>	<u>Page</u>
INTRODUCTION	1
EXPERIMENTAL METHOD	3
Molecular N <sub>2</sub> Beam	3
Target Chamber	5
Ion Collection and Current Measurements	8
Consistency Checks and Systematic Corrections	8
RESULTS	11
DATA RELIABILITY	18
DISCUSSION	20
REFERENCES	21

## ILLUSTRATIONS

<u>Figure</u>		<u>Page</u>
1	Block Diagram of Apparatus	6
2	Target Configurations	6
3	Ionization Cross Sections for Nitrogen on Argon as Functions of Kinetic Energy in the Center-of-Mass System	12
4	Ionization Cross Sections for Nitrogen on Oxygen as Functions of Kinetic Energy in the Center-of-Mass System	13
5	Ionization Cross Sections for Nitrogen on Nitric Oxide as Functions of Kinetic Energy in the Center-of-Mass System	14
6	Ionization Cross Sections for Nitrogen on Argon as Functions of Available Energy above Threshold	15
7	Ionization Cross Sections for Nitrogen on Oxygen as Functions of Available Energy above Threshold	16
8	Ionization Cross Sections for Nitrogen on Nitric Oxide as Functions of Available Energy above Threshold	17

## INTRODUCTION

The process of ionization has important consequences in many areas pertinent to hypersonic flight and atmospheric entry, with their attendant extremes in temperature. Measurements of bulk ionization rates are difficult in many regimes of chemical species, pressure, and temperature. At best, the results tend to be gross and to yield little information on detailed ionizing processes. It is thus of interest to develop a model for bulk ionization, from which bulk ionization rates can be calculated. Recently, Hansen<sup>(1)</sup> formally proposed such a model, recognizing that ionization processes between excited collision partners would be an extremely important part of it. His model directly employs kinetic theory in terms of cross sections for ionization, and the reaction rate is determined by straightforward integration over all ionizing collisions. The important feature is that collisions between internally excited collision partners are not ignored, as they were previously. The major difficulty encountered in validating this model has been the lack of information regarding the ionization cross sections. Although a few cross-section values for neutral-neutral ionization between ground-state collision partners were available, none had been measured for collisions between excited partners. The present research was initiated to measure a few representative cross sections in this category.

Recently it was found<sup>(2)</sup> possible to produce a fast neutral beam of  $N_2$  molecules in the  $A^3\Sigma_u^+$  state (6.3 eV). Since  $N_2$  is a species of some practical importance, and since the A-state has a sufficiently high internal energy to produce observable effects, it was decided to employ  $N_2(A)$  as the beam species. For targets, Ar atoms and  $O_2$ , NO, and CO molecules were picked as representative and tractable.

The apparatus for producing a nitrogen molecular beam has been described in detail.<sup>(3)</sup> It utilizes production of nitrogen molecular ions by electron

bombardment (22 eV electrons), electrostatic acceleration of the ions into a beam having the desired energy and trajectory, and their neutralization by charge transfer in a suitable gas. Nitrogen has usually been selected as the neutralizing gas because the resonant character of the interaction leads to production of fast ground-state neutrals with a large cross section at low energy. Hydrogen has also been employed, although it is not quite resonant and thus has a smaller charge-transfer cross section at the lowest energies. However, hydrogen has the advantage that the kinetic energy available for excitation (center-of-mass energy) in  $N_2^+ + H_2$  collisions is only 1/15 the beam energy, thus putting a limit on the internal excitation which might be present in the  $N_2$  molecular beam.

For the excited beam employed here, nitric oxide was used as the neutralizing gas (bar indicates the fast particle), i. e. ,



The charge-transfer cross section for these reactants has been measured to be about one-fourth that for  $N_2^+$  in  $N_2$  (i. e. , about  $9A^2$  at 30 eV). Most significant is the observation that it appears to increase with decreasing energy to below 20 eV, suggesting that a resonant or near-resonant process occurs. A plausible explanation can be found in the energy balance of reaction (1). The  $N_2^+$  has an ionization energy of 15.58 eV and the  $NO^+$ , 9.27 eV, a difference of 6.31 eV. This is very close to the energy of the metastable  $A^3\Sigma(v=1)$  state of  $N_2$ . Reaction (1) is essentially resonant if this is the excited state populated during the charge transfer. Capture into other states of the nitrogen molecule (except for other low-lying vibrational levels of the  $A^3\Sigma$  state) would be significantly nonresonant. Furthermore, if other nearby electronic states were to be populated during the collision, some of these (such as the important  $B^3\Pi$  state) would decay to the  $A^3\Sigma$  level. Transitions from the  $N_2^+$  to the  $A^3\Sigma$  state of  $N_2$  are compatible with the application of the Frank-Condon principle, and the spin-conservation rule is not violated.

The ionization cross sections for  $N_2^* + Ar$ ,  $O_2$ , and  $NO$  collisions were measured in the same manner described previously<sup>(4,5)</sup> for  $N_2 + N_2$  and  $N_2 + O_2$  collisions. The fast excited molecular beam traversed a low-pressure gas target ( $10^{-4}$  torr) between the guarded plates of a parallel-plate ionization chamber. Negative charges arising from ionizing collisions were driven to the collector plate by the electrostatic field between the plates. Particular care was taken to exclude stray secondary electrons ejected by scattered beam molecules. Knowledge of the target number density, collector length, current of negative charges, and neutral beam intensity allowed a determination of the ionization cross section (more precisely, the total cross section for production of negative charges in the collisions). The target number density was determined from the target gas pressure. Ideally, the neutral beam intensity could be inferred from the current of slow ions produced in the charge-transfer cell, since each slow ion corresponded to a fast neutral molecule. In reality, some scattering occurred, and a small, measured correction to the neutral beam intensity was applied.

## EXPERIMENTAL METHOD

### Molecular $N_2$ Beam

The molecular  $N_2$  beam apparatus has been discussed in detail elsewhere.<sup>(3)</sup> A short summary will be given here.

Figure 1 shows a block diagram of the beam-producing apparatus. An  $N_2^+$  ion beam was produced by the ion source and lens system. The ion source was operated as an electron impact source. The electron energy was normally 22 eV. The lens system determined the final ion beam energy and focused the ion beam through the apertures behind it. A fraction (< 20%) of the ion



beam entering the neutralization chamber was neutralized by charge transfer with  $N_2$  or  $H_2$  gas (or NO for the excited beam). The mixed ion and molecular beam passed between deflecting plates where the remaining ions were removed.

The molecular  $N_2$  beam intensity was determined by measuring three currents as follows. The ion collector current was  $i_1$  and corresponded to those ions which had not undergone charge transfer or strong scattering. The current  $i_2$  arose from the charge-transfer cup which was held at a potential positive enough to repel the slow ions arising from charge transfer, but not positive enough to repel scattered ions;  $i_2$  therefore corresponded to ions strongly scattered which had not undergone charge transfer. The ions arising from charge transfer were driven by the positive cup to the grid and were collected as  $i_3$ . Now  $i_1 + i_2 + i_3$  was the total ion current entering the neutralization chamber. Thus  $\beta$ , the fraction of all entering ions which underwent charge transfer, was given by

$$\beta = \frac{i_3}{i_1 + i_2 + i_3} \quad . \quad (2)$$

If  $I$  represents the unscattered ion beam in the event charge transfer had not occurred, the current  $i_1$  was given by

$$i_1 = I - \beta I \quad ,$$

or

$$I = \frac{i_1}{1 - \beta} \quad . \quad (3)$$

It follows that the molecular beam intensity in molecules per second,  $B$ , was

$$B = \beta I = \frac{\beta i_1}{1 - \beta} = \frac{i_3}{1 + i_2/i_1} \quad , \quad (4)$$

where the currents are in ions per second.

It is seen that if no scattering were present ( $i_2=0$ ), the molecular beam intensity would have been equal to  $i_3$ , the slow ion current. A more detailed discussion of the assumptions implicit in Eq. (4) has been given previously.<sup>(3)</sup>

It was also shown in that reference that the absolute intensity could be determined to within 20% by the use of this method. Beam intensities of the order of  $10^9$  molecules per second were used in this work.

The molecular  $N_2$  beam energy and energy spread were obtained by first measuring the energy and energy spread of the  $N_2^+$  ions entering the neutralization chamber. In order to determine the energy spread and average energy of these  $N_2^+$  ions, the neutralization chamber was used as a Faraday cage. With no neutralizing gas present, the grid and cup were connected together and formed the collector for the Faraday cage. High positive potentials were placed on both the repeller and ion collector in order to electrically close the exit aperture of the cup. The electrode at the entrance aperture of the cup was maintained approximately two volts negative with respect to the equipotential region in front. This focused entering ions away from the aperture edges and thus minimized edge effects caused by changing the Faraday-cage collector potential. A plot of the Faraday-cage collector current as a function of its potential indicated an energy spread at half-maximum of 0.4 eV. The average energy was 1.8 eV less than the ion source-to-neutralization region potential difference. This discrepancy might have been a small ion-source offset caused by the extraction field, or a contact potential difference between the ion source and neutralization region. Molecular beam energies in this work were determined under the assumption that negligible momentum was transferred during charge transfer, and therefore that the neutral beam energy was the same as the ion beam energy. A correction of 1.8 eV was made to the beam energy as discussed above.

### Target Chamber

Configuration A in Figure 2 shows the electrode arrangement in the target chamber. The molecular  $N_2$  beam was directed between the grid and the collector and guard plate in a direction parallel to the grid wires. The purpose of the grid was to suppress secondary electrons arising at the back plate

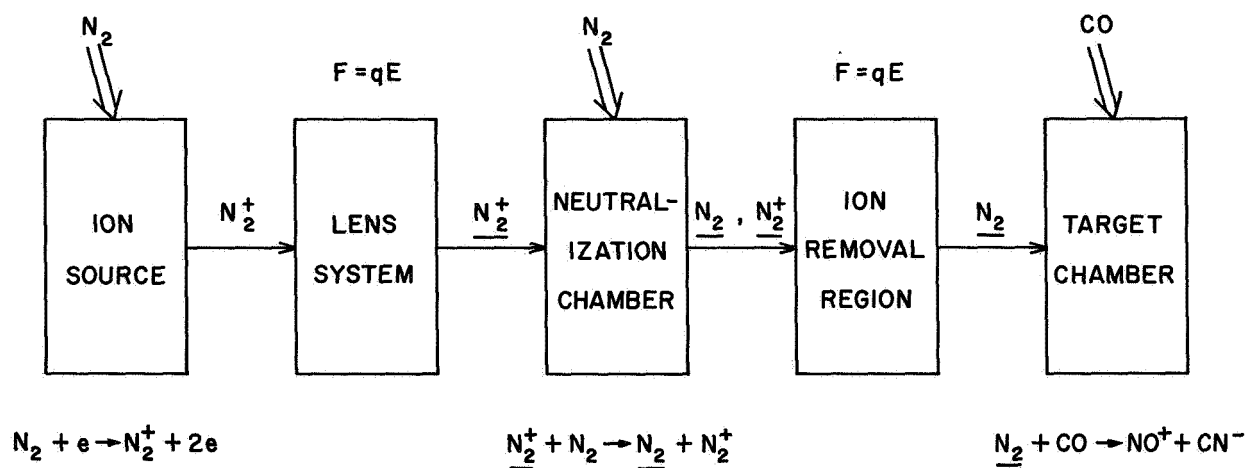


Figure 1 Block Diagram of Apparatus

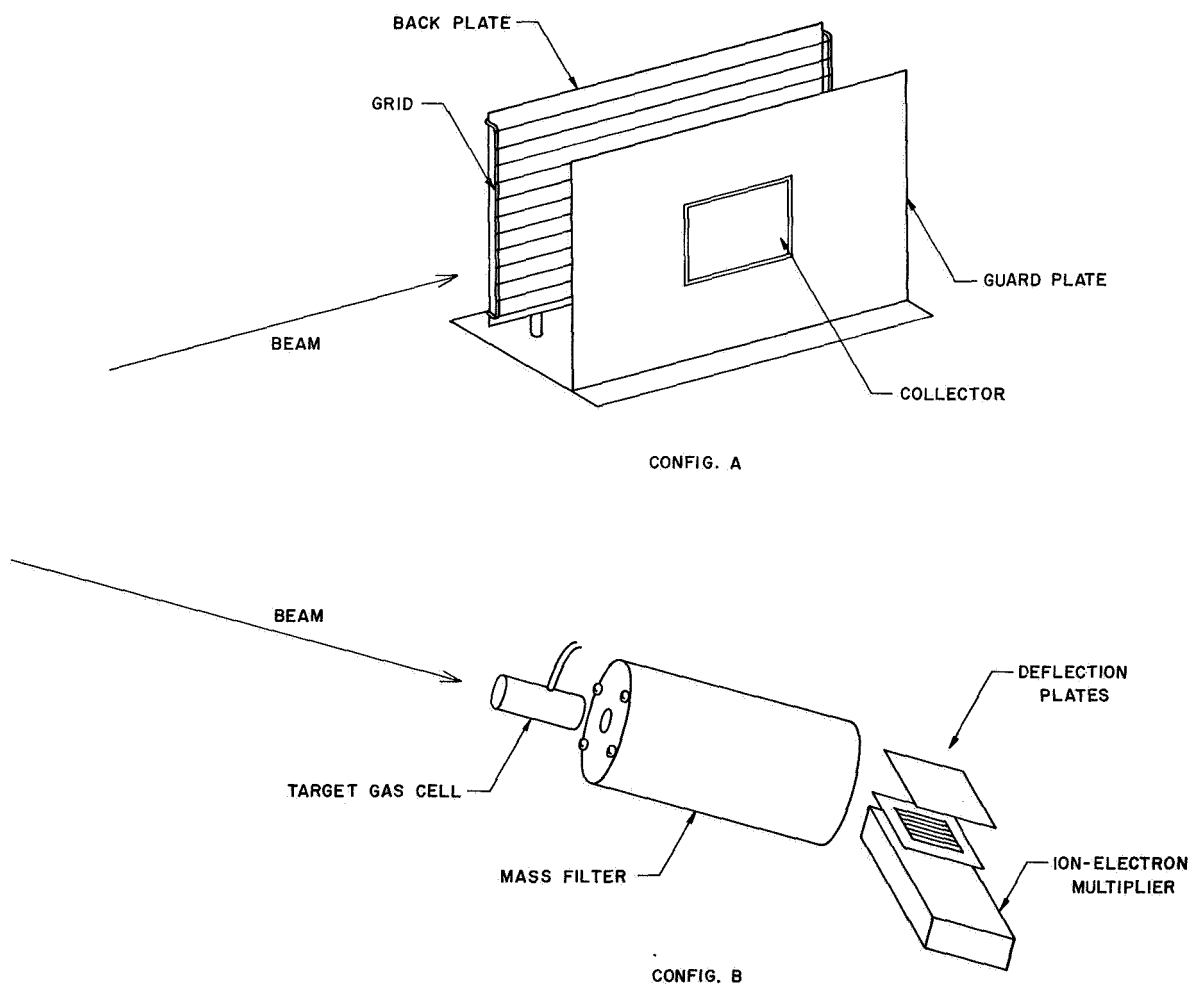


Figure 2 Target Configurations

behind the grid due to scattered molecules. The grid was composed of 0.0008-inch-diameter gold-plated tungsten wires spaced about 0.2 inch apart. It therefore presented a very small solid angle for molecules scattered out of the beam. A potential difference of 360 volts was maintained between the back plate and grid. This prevented secondary electrons arising at the back plate from reaching the collector. The grid-to-collector potential difference was normally 600 volts. The guard plate insured a uniform field over the collection region and a well-defined collection length. The collector was 10x4 cm, and was spaced 4 cm from the grid. The grid was spaced 1 cm from the back plate. All electrode surfaces were plated with gold.

The electrode assembly was contained in the target chamber, which was evacuated by means of a 6-inch liquid-nitrogen-trapped mercury diffusion pump. The only connection between the beam vacuum system and the target chamber vacuum system was the 3mm exit aperture from the neutralization chamber. This arrangement was used so that the target chamber pressure could be controlled independently of the neutralization chamber pressure. Furthermore, when a target gas different from the neutralizing gas was used, it was essential to keep the target gas as pure as possible. This necessitated continually pumping out the nitrogen,  $H_2$ , or NO which entered the target chamber from the neutralization chamber.

Target gas was admitted continuously to the target chamber through an aperture pointed so that the gas in the interaction region had diffused off the chamber walls. In this way the pressure gradient in the interaction region was kept small. The pressure calibration was made with a McLeod gauge, an ion gauge, and a capacitance manometer.<sup>(6)</sup>

The gas purity for  $N_2$ , Ar,  $O_2$ , NO, and CO was 99.99, 99.999, 99.99, 99.92 and 99.97, respectively.

### Ion Collection and Current Measurement

The collecting field was maintained between the grid and the collector and guard plate. The distance between was 4 cm. The collector and guard plate were held at ground (chamber) potential, with the grid being made negative. A negative potential of a few hundred volts on the grid sufficed to repel the electrons and negative ions to the collector. Relatively few positive ions then reached the collector, since their energies would have had to be quite high and their directions correct to overcome the field.

The collector plate was connected to a Cary vibrating-reed electrometer driving a strip-chart recorder. It was possible to reliably measure currents smaller than  $10^{-16}$  ampere when charging times of 100 seconds were used.

### Consistency Checks and Systematic Corrections

A series of consistency checks which has been developed was applied in each set of cross-section measurements. In some cases systematic errors were found and the necessary corrections were obtained in these checks. The techniques have been previously discussed in detail,<sup>(4, 5)</sup> but will be briefly reviewed here. The checks involve collecting field saturation, target pressure saturation, grid efficiency, beam energy-offset in cup, charge transfer slow-ion-current errors, neutralizing gas pressure saturation, and gas mixing effects.

Collecting field saturation was not difficult to achieve in the present work. With a potential of 180 volts on the grid (collector and guard plate grounded) the collected current was within 10% of its value with 900 volts. Essentially no change occurred between 300 and 900 volts. Except during this check, the grid was operated at 600 volts.

The pressure saturation measurements consisted of cross-section measurements taken at several target pressures between 0.5 and  $7.5 \times 10^{-4}$  torr. The

usual decrease in cross section was observed with increasing target pressure due to target gas scattering. The normal pressure for measurement was  $1.3 \times 10^{-4}$  torr, and at that pressure the decrease amounted to only a few percent. No large secondary electron effects were observable.

Grid efficiency presented no problem in this work, and was quite adequate. Any secondary electrons arising from the impact of gas-scattered molecules on electrode surfaces gave rise to a current which had the same pressure dependence as the ionization current. It was therefore not possible to separate this secondary current by varying the pressure. The magnitude of this particular effect was determined in the following manner. If no grid had been present, secondary electrons arising at the back plate due to the impact of gas-scattered molecules would have been accelerated to the collector and would have been indistinguishable from ionization electrons. The grid was added to eliminate this effect. By making the grid sufficiently negative, it was possible to return the secondary electrons to the back plate. However, the grid itself presented a non-zero area to scattered molecules, and secondary electrons arising at the grid could reach the collector. The grid wires constituted about 0.5 percent of the total grid area as seen by scattered molecules. With the grid in operation, the secondary current should therefore have been less than one percent of the current present without the grid. Measurements were made with the grid 0 and 360 volts negative with respect to the back plate (grid-to-collector potential difference = 600 volts). At zero difference in potential, the secondary current should have been about a factor of 100 greater than when the grid was repelling the secondaries arising at the back plate. It was found that with the back-plate-to-grid potential at zero volts, the ionization current less than doubled, indicating that electrons from the grid and back plate could be ignored under usual operating conditions.

A slight beam-energy offset occurs normally in the cup due to the method of monitoring the beam intensity. The grid does not completely shield the region

within it from the cup potential, and the ions are thus normally neutralized in a region of varying potential. This effect may be eliminated if necessary by first measuring  $\beta$  and then making the cup potential zero during the ionization measurement. This does not interfere with the measurement of  $i_1$ , and the beam intensity can therefore still be determined from Eq. (4). This method was used in determining the effective energy offset near threshold for each cross section. It amounted to about 2.0 eV in terms of beam energy, but was easily corrected for.

Since the neutral beam intensity is determined by measuring the current of slow ions produced in the neutralizing gas cell and assuming that each slow ion corresponds to a fast neutral, it is necessary to make an energy analysis of the slow ions in order to consider properly the scattered ions resulting from hard collisions. For previous work involving ground-state beams, this energy analysis was fairly unambiguous due to the large charge transfer cross sections obtained. In the present work on excited beams and charge transfer in NO, the analysis was not as clear, and the possible scattering unaccounted for might have produced as much as a 20% error in the beam intensity. More will be said on this later.

The neutralizing gas pressure was varied by a factor of two to find how much neutral beam scattering and quenching might be occurring due to the neutralizing gas. It was found that at the  $\beta$ 's normally used, the effect was less than 10%.

Gas mixing effects necessitated the largest corrections in the present work, but the corrections should have been quite reliable. These effects refer to the NO neutralizing gas present in the target gas due to leakage from the neutralization cell into the target chamber, and from target gas present in the neutralization cell due to leakage in the opposite direction. The NO in the target was quite serious because of the large  $N_2^* + NO$  cross section at a given beam energy. The target gas in the neutralization cell was serious because of

the high transfer cross section in the target gas, yielding ground-state beam molecules. These effects could be corrected for by making three separate measurements at each energy: one without target gas but with neutralizing gas, another with target gas but without neutralizing gas, and a third with both target gas and neutralizing gas. By combining these results properly, corrections could be made, which ranged from a few percent to as high as 30%.

## RESULTS

Ionization cross section values (more precisely, total cross sections for negative charge production),  $\sigma_i$ , were obtained from

$$\sigma_i = 3.05 \times 10^{-20} (i/PB) \text{ cm}^2, \quad (5)$$

where  $i$  is collector current in units of  $10^{-16}$  amp,  $P$  the target pressure in units of  $10^{-4}$  torr, and  $B$  the neutral-beam equivalent current in units of  $10^{-10}$  amp. The collector length was 10 cm and the temperature was  $22^\circ\text{C}$ .

The threshold behavior of the measured cross sections as functions of available (center-of-mass) kinetic energy are shown in Figures 3, 4, and 5.

Curves labeled A in these plots depict the results when  $\text{N}_2$  or  $\text{H}_2$  was employed as the neutralizing partner (ground-state) and curves B are those obtained from neutralization by NO (excited-state). The effect of the internal energy is readily seen.

Figures 6, 7, and 8 show the results obtained over a larger energy range. Note that both cross section and available energy are here displayed on logarithmic scales. Curves A are for ground-state  $\text{N}_2$  molecules and curves B are for excited  $\text{N}_2$  molecules. The abscissa values in these cases represent kinetic energy in the center-of-mass system minus the minimum ionization energy threshold. Curves C show the same data as curves B, except that the



energy scale is shifted by adding 6.3 eV for the excitation energy to the kinetic energy. Thus a zero abscissa value corresponds to the actual total energy threshold in curves A and curves C. Curves B show essentially the effect of ignoring the excitation energy.

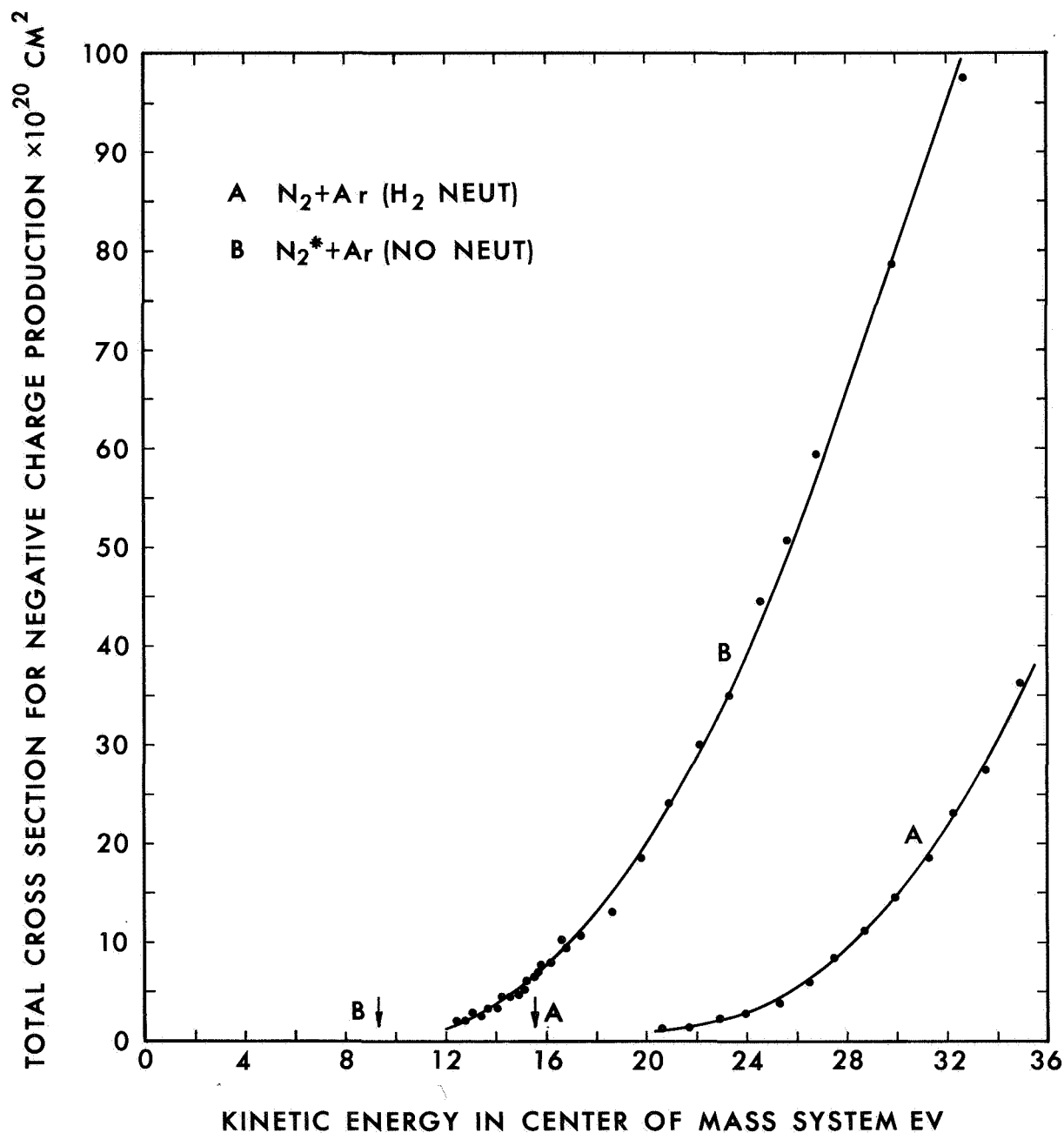


Figure 3 Ionization Cross Sections for Nitrogen on Argon as Functions of Kinetic Energy in the Center-of-Mass System. Arrows indicate threshold corresponding to each curve.

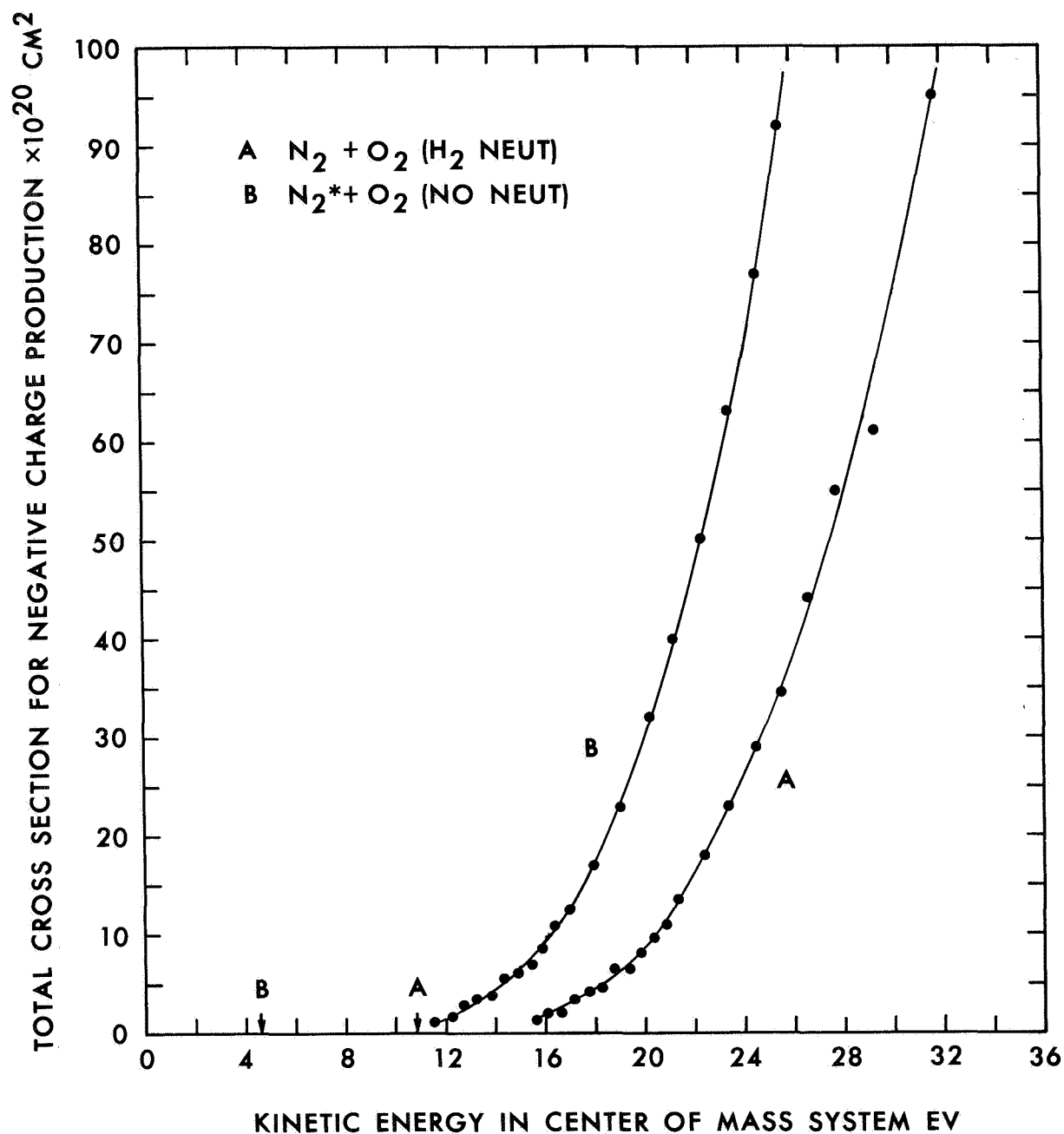


Figure 4 Ionization Cross Sections for Nitrogen on Oxygen as Functions of Kinetic Energy in the Center-of-Mass system. Arrows indicate threshold corresponding to each curve.

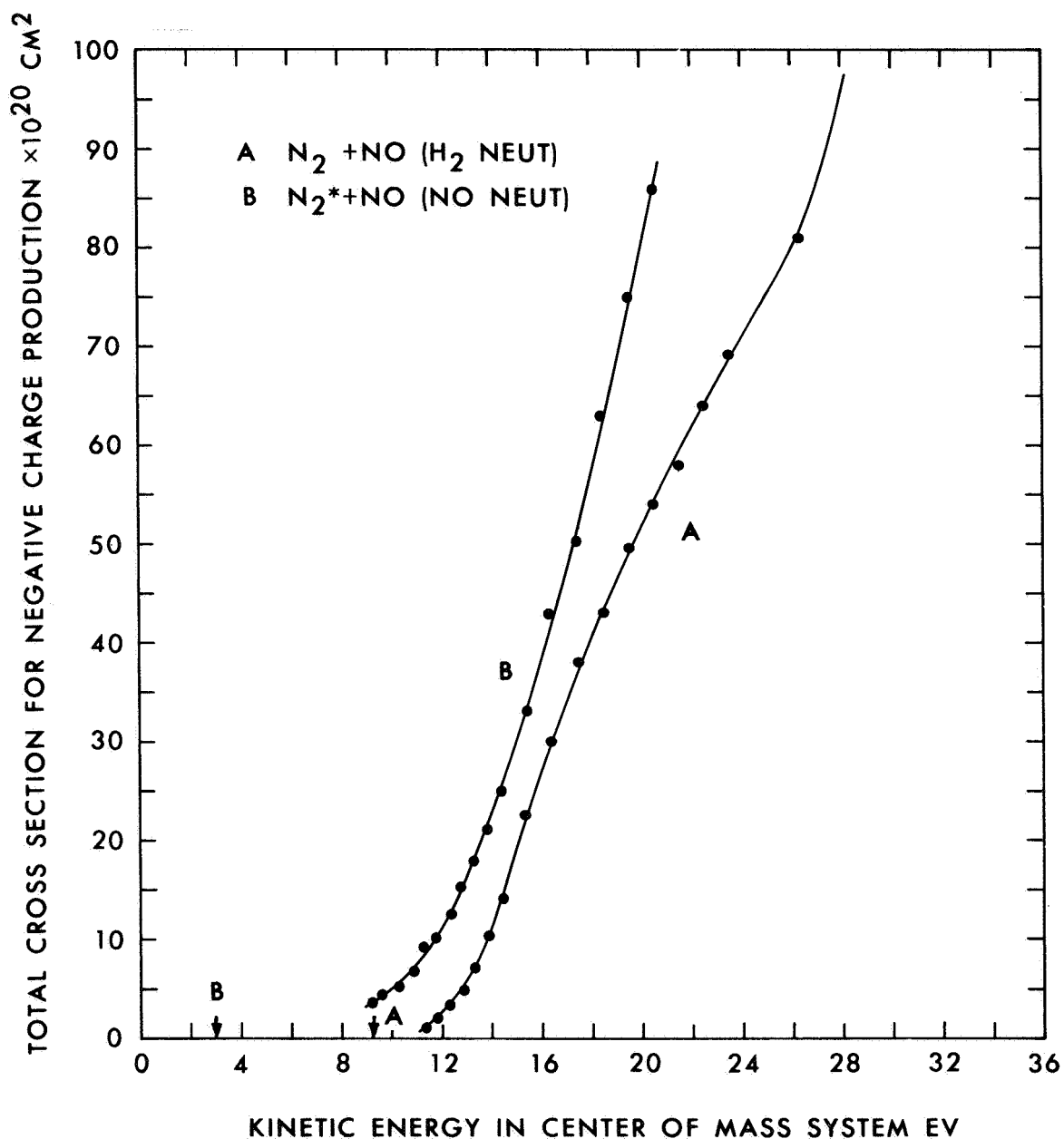


Figure 5 Ionization Cross Sections for Nitrogen on Nitric Oxide as Functions of Kinetic Energy in the Center-of-Mass System. Arrows indicate threshold corresponding to each curve.

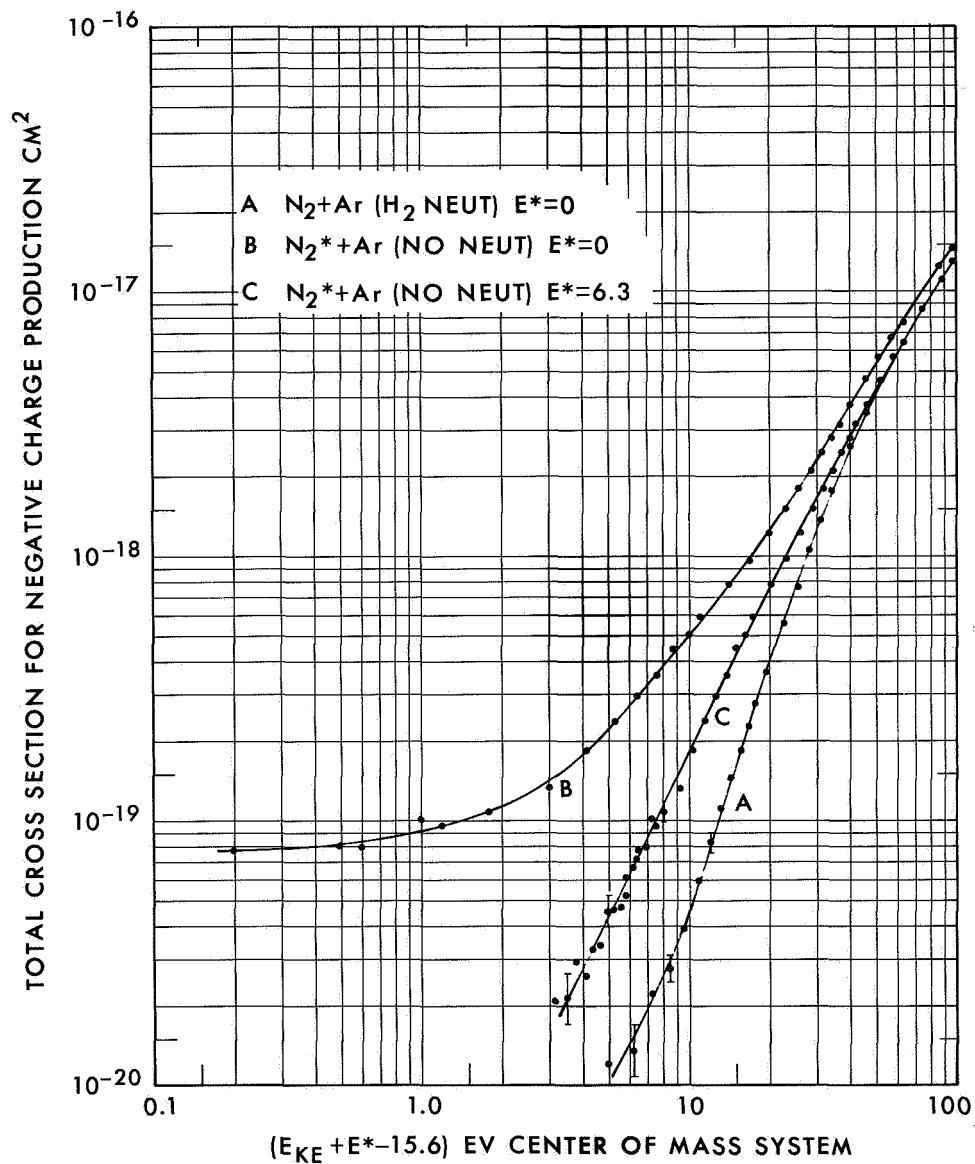


Figure 6 Ionization Cross Sections for Nitrogen on Argon as Functions of Available Energy above Threshold, Curves A and C. Curve B shows the effect of ignoring internal energy in the "excited" beam.

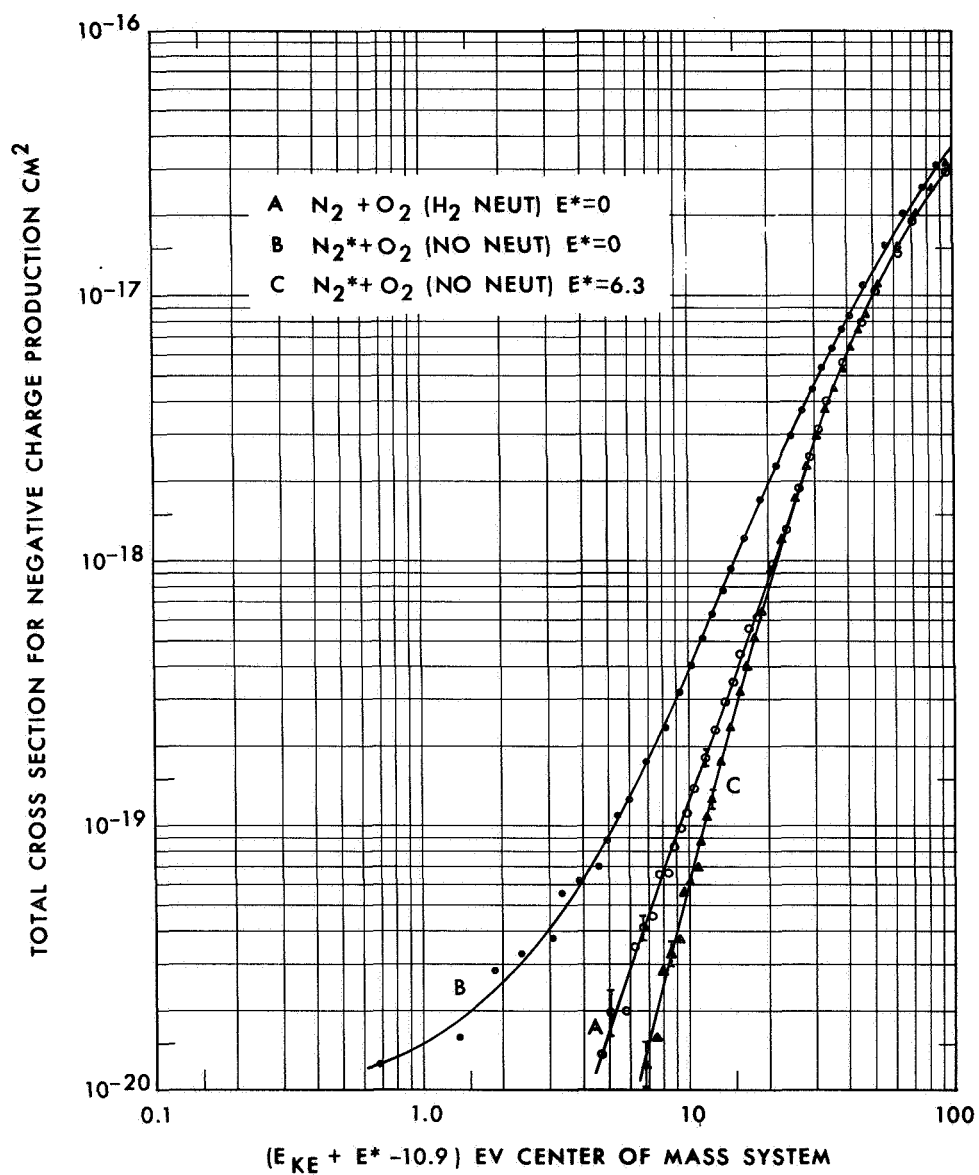


Figure 7 Ionization Cross Sections for Nitrogen on Oxygen as Functions of Available Energy above Threshold, Curves A and C. Curve B shows the effect of ignoring internal energy in the "excited" beam.

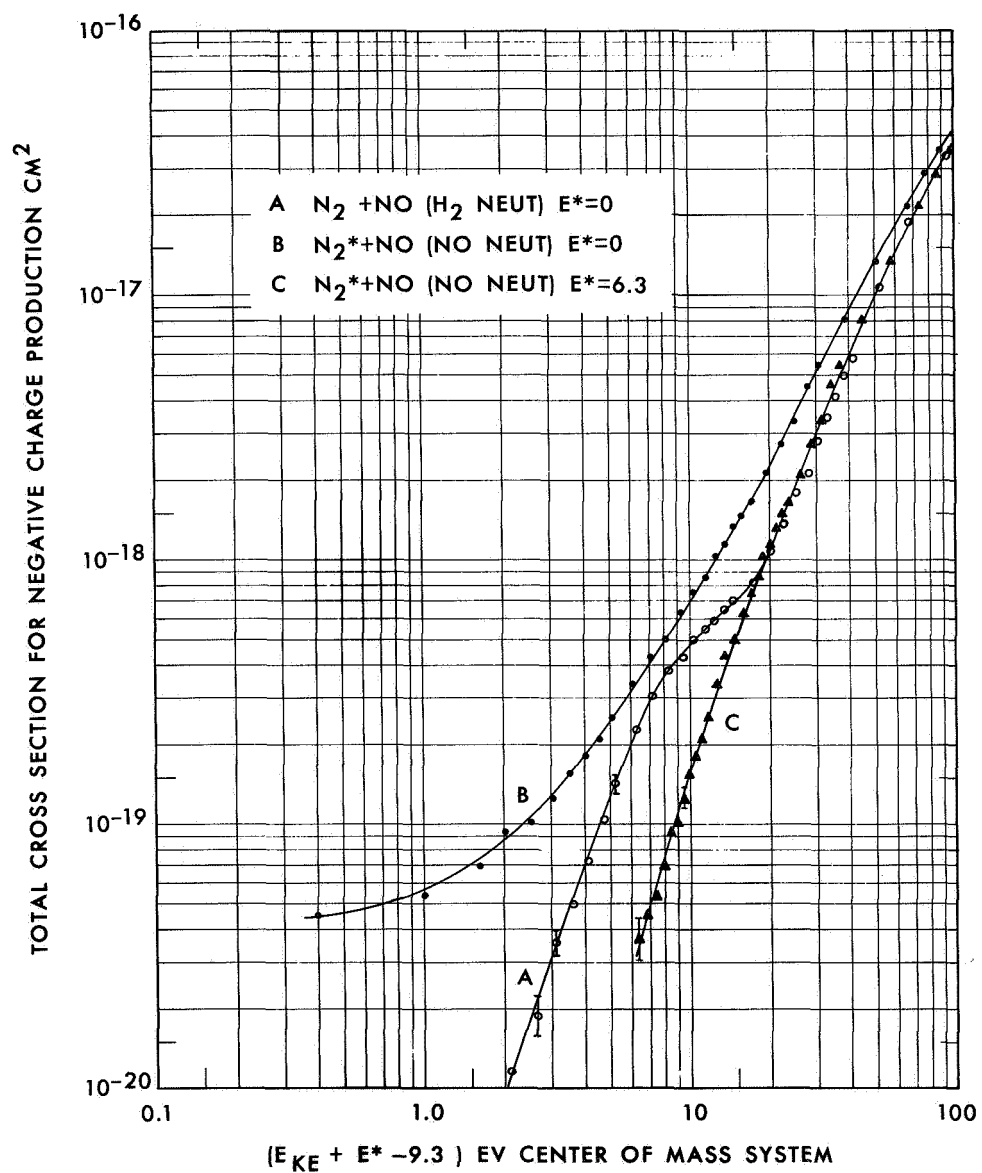


Figure 8 Ionization Cross Sections for Nitrogen on Nitric Oxide as Functions of Available Energy above Threshold, Curves A and C. Curve B shows the effect of ignoring internal energy in the "excited" beam.

## DATA RELIABILITY

The bars on curves A and C of Figures 6, 7, and 8 represent random uncertainties in the data. They were largest at low energy because of the small signal currents obtained, and decreased to less than  $\pm 10\%$  at high energies. Beam energy uncertainty also became important near threshold, but was estimated to have been less than 0.3 eV in the center of mass system.

In regard to systematic errors in the measurement of the quantities entering Equation (5), the measurements of  $i$  and  $P$  should have been accurate to a few percent. The largest potential systematic error arose from uncertainty in the neutral-beam intensity,  $B$ . Although the total neutral beam intensity was believed known<sup>(3)</sup> to within  $\pm 20\%$ , the fraction of excited molecules in the excited beam is in some doubt. The data presented here have been reduced under the assumption that the excited beam consisted entirely of excited molecules. While it may be argued that, on the basis of almost-resonant charge transfer, the excited  $N_2 A^3 \Sigma_u^+$  should be highly preferred, the possibility exists that some ground-state  $N_2$  molecules are produced. The possibility of higher-lying excited states must also be considered, particularly in view of recent measurements which indicate that some of the initial  $N_2^+$  electronic states may have lifetimes long enough to be present in the ion beam.

To explore these possible errors in intensity of the excited-beam, the ion-source ionizing electron energy was varied from 17 to 26 eV at given ion beam energies. No effect on the results was observed for ground-state beam measurements. However, marked effects were noted for  $N_2^*$  incident on Ar,  $O_2$ , NO, and a gold surface. In each case a rapid rise (about a factor of two) in the apparent cross section (or secondary emission coefficient) near threshold occurred in changing electron energy from 17 to 19 eV. Furthermore, the shapes of all four cross section vs electron energy curves were very similar from 17 to 20 eV. This is significant since the thresholds for charge production

are 15.6, 10.9, 9.3 and 5 eV, respectively. The first hypothesis made to explain this was that the ratio of excited-state to ground-state molecules was changing with vibrational or electronic populations in the  $N_2^+$  ions, which in turn changed due to the changing electron energy. Thus at 17 eV the beam should have been largely ground-state. But this hypothesis could not entirely explain the observations, which was made clear by comparing  $N_2^* + NO$  cross-section vs kinetic-energy curves (Figure 8, curve C) taken at different electron energies. Since the ground-state curve shows distinct structure, a preponderance of ground-state molecules in the "excited" beam would have shown similar structure. However, the curve for 17eV electrons showed only a hint of structure. An analysis put a limit of about 25% ground-state molecules in the "excited" beam. Thus this hypothesis could at best only partially explain the results.

Other possibilities are that, at lower electron energies, an ion source impurity is showing up which charge-transfers in NO but produces less ionization. The ratio of impurity to  $N_2^+$  would decrease sharply as the electron energy was raised above the  $N_2^+$  threshold. It is intended at another time to check the purity of the ion beam as a function of electron energy. A further possibility is that an ion-molecule reaction occurs which is dependent on electron energy and which produces a slow ion in the neutralization chamber but no ionization in the target chamber.

The results up to now, along with the interpretations considered, suggest that, although the effect of varying the electron energy has not been satisfactorily explained, the results obtained with 22eV electrons are not grossly in error. For example, although the cross section for  $N_2^* + Ar$  changes markedly below 22eV electron energy, it changes almost none from 22 to 26 eV. One must, of course, continue to recognize the possibility of error until further work yields a satisfactory explanation.

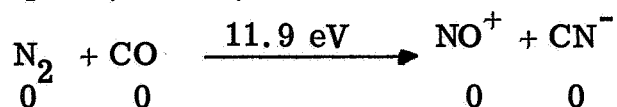


Effects of higher-lying metastable states can also be seen by varying the electron energy. Thus, above 22eV electron energy, the  $N_2^* + O_2$  ionization cross section rises abruptly. Up to that point, the shape of the curve is very similar to  $N_2^* + Ar$ . This is interpreted as being due to metastable  $N_2$  beam molecules with energy sufficient to "Penning ionize" the  $O_2$ . A ratio of one in  $10^4$  of such highly excited molecules in the beam would explain the rise. So long as 22eV, or lower, electrons are used, this effect should cause no problem. A similar and more serious problem arose for  $N_2^* + NO$ . In this case, with its 9.3eV threshold, high-lying metastables were noticeable above 19 eV electron energy.

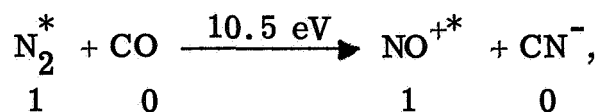
The above effects are most serious near threshold where the cross sections are small. It seems unlikely from the results obtained up to now that the errors could be greater than a factor of 2 even at the lower end of the curves, and more likely that the results are good within  $\pm 35\%$ .

## DISCUSSION

In addition to the marked increase in cross section at a given kinetic energy due to internal energy, a particularly striking feature of the present results is the change in shape of some of the curves for the excited beam relative to the ground-state beam. This change is especially noticeable with  $N_2^* + NO$  and  $N_2 + NO$ , where the ground-state case shows structure and the excited-state case does not. Since many separate ionizing processes are undoubtedly being summed in these "total" cross sections, it would be surprising if no selection rules other than total available energy were operative; indeed another rule has apparently been found in one case so far,  $N_2^* + CO$ , where the internal energy appears to be almost ineffective in increasing the cross section. This can be explained on the basis of spin-selection rules. The process involved in  $N_2 + CO$  has spins (beneath)



and therefore spin is conserved. If the  $N_2^*$  is  $A^3\Sigma$ , then spin is not conserved unless



and the kinetic energy threshold is reduced only 1.4 eV by the internal energy. This is consistent with the observed results. Since these results are somewhat preliminary, they are presented here not as a complete explanation, but as a working hypothesis. These spin rules do not appear to limit the processes which have been considered so far for  $N_2^* + NO$ , and at this time no satisfactory explanation for the shape changes can be claimed.

In this regard, further work toward mass-spectrometrically determining<sup>(7)</sup> the reaction products should be of great value. (See Figure 2, Configuration B). For example, the processes  $N_2 + CO \rightarrow NO^+ + CN^-$  and  $N_2 + O_2 \rightarrow NO^+ + (NO^-)$ , with thresholds 11.9 and 10.9 eV as used here, could not have been confirmed without mass identification. It would now be of interest to determine whether  $N_2^* + CO$  and  $N_2^* + O_2$  produce the same reactions in the same abundance as ground-state  $N_2$  molecules.

## REFERENCES

1. C.F. Hansen, Proceedings of the Sixth International Symposium on Rarefied Gas Dynamics, M.I.T. 1968, Academic Press, 1969.
2. N.G. Utterback and B. Van Zyl, Phys. Rev. Letters 20, 1021 (1968).
3. N.G. Utterback and G.H. Miller, Rev. Sci. Instr. 32, 1102 (1961).
4. N.G. Utterback and G.H. Miller, Phys. Rev. 124, 1477 (1961).
5. N.G. Utterback, Phys. Rev. 129, 219 (1963).
6. N.G. Utterback and T. Griffith, Jr., Rev. Sci. Instr. 37, 866 (1966).
7. N.G. Utterback, J. Chem. Phys. 44, 2540 (1966).